Nucleation in a time-dependent Ginzburg-Landau model: A numerical study

Oriol T. Valls
School of Physics and Astronomy and Minnesota Supercomputer Institute, University of Minnesota, Minneapolis, Minnestoa 55455

Gene F. Mazenko
The James Franck Institute and the Department of Physics, The University of Chicago, Chicago, Illinois 60637

(Received 26 March 1990)

We study the nucleation of the stable phase in a time-dependent Ginzburg-Landau model with an asymmetric double-well structure. The system is taken to be initially in the metastable phase and is then driven toward stable equilibrium by thermal noise or by randomness in the initial conditions. Results are presented as a function of the field h, which splits a pair of degenerate minima, and the noise strength or dispersion in the initial field values. Over the rather wide range of parameter values that we have considered, we find that the nucleation rate can be fairly accurately described by an activated form. The activation energy is a stronger function of h for intermediate values of h than predicted by classical theory, and it is a weak analytic function of noise strength.

I. INTRODUCTION

The process of nucleation is central to the evolution of a metastable state towards its final stable equilibrium state. Classical nucleation theory[1] was pioneered for fluid systems by Becker and Döing.[2] Subsequent theoretical development[3,4] focused on simple field-theoretical models governed by effective Ginzburg-Landau-Wilson (GLW) Hamiltonians. Cahn and Hilliard[5] and Langer[6] worked out, in detail, the dynamics of a nucleating droplet in an undercooled background in the context of a time-dependent Ginzburg-Landau (TDGL) model. In this paper we discuss the direct numerical solution of this Langevin model in the appropriate metastable circumstances. Our results are qualitatively consistent with the classical results of an activated nucleation rate and give estimates for the range of validity of the weak-field and low-temperature limits where analytic results exist.

Direct comparison between nucleation theory and related experiments has been difficult.[7] Nucleation experiments in fluids are complicated by a number of factors not present in the simple GLW models and it is difficult to check quantitative details of the theory. It seems clear that it is desirable to have a direct check of the classical theory in the context of the simple TDGL model. Somewhat surprisingly, there has not been a direct confrontation between the classical theory and direct numerical simulation of the models for which the classical theory has been established in detail. One of the main motivations of this paper is to provide a set of numerical results for the TDGL model against which theoretical results can be compared in the future. Early simulational efforts[8] on unstable and metastable systems focused on kinetic Ising models. Unfortunately it is difficult to make a direct connection between kinetic Ising models and the TDGL models treated by the usual field theories. The statistical problem of rare nucleation events in the kinetic Ising model seems to account for the lack of any systematic studies of nucleation rates. In our work here we describe a systematic numerical study of the TDGL model over a substantial range of parameters.

We study the classic nucleation problem. Consider a field $\psi(\mathbf{x})$, which is a function of position, governed by an asymmetric double-well potential $V(\psi)$ with a metastable minimum at $\psi=\psi_-$ and a stable minimum at $\psi=\psi_+$. It is assumed that the energy difference between the two states

$$\Delta V = V(\psi_-) - V(\psi_+) > 0$$

is governed by an asymmetry parameter h. In the case of a "ϕ^4" field theory, h is simply an applied magnetic field or chemical potential favoring the ψ_+ state. The procedure that we follow is to place, at some time $t=t_0$, the system in a state where, on average, $\langle\psi\rangle\approx\psi_-$. Thus, we have prepared our system in a metastable state. We discuss in Sec. II the various ways in which we prepare this initial state. One is then interested in the length of time it takes for the stable phase to nucleate in the system, driven by thermal noise or initial random fluctuations, and for the system to find its way to the final stable equilibrium state near ψ_+.

Our results are qualitatively clear. The nucleation rate is of the expected general form

$$\tau = \tau_0 e^{E/\varepsilon} , \tag{1.1}$$

where ε is a dimensionless measure of the randomness driving the system (the temperature or the variance in a random Gaussian initial distribution) and E is the associated activation barrier which is a weak analytic function of ε as $\varepsilon\to 0$. τ_0 is also found to be a weak but not analytic function of ε as $\varepsilon\to 0$. We also find the activation energy E has a strong field (h) dependence. As $h\to 0$ the field dependence appears to be compatible with the predictions of the classical theory, $E\sim h^{-(d-1)}$ in d spatial dimensions. For larger values of h, where the classical theory need not be valid, we find a much stronger variation of E with h than predicted by the classical theory.

II. MODEL AND METHODS

As explained in the Introduction, we will study in this paper the simplest Langevin model for the dynamics of a system evolving from a metastable towards a thermodynamically stable state. The static properties of our system are determined by a GLW effective Hamiltonian

$$\tilde{F}=\int d^d x' \left[-\frac{r}{2}\phi^4+\frac{u}{4}\phi^4+\frac{K}{2}(\nabla\phi)^2-H\phi \right] , \quad (2.1)$$

where $\phi(\mathbf{x}',t)$ is a scalar field variable. We define the rescaled variables

$$\psi(\mathbf{x}',t)=\left[\frac{u}{r}\right]^{1/2}\phi\left[\left[\frac{K}{r}\right]^{1/2}\mathbf{x}\right],$$

$$F=\tilde{F}u/r^2 ,$$

$$h=Hu^{1/2}/r^{3/2} ,$$

and we take the quantity $(K/r)^{1/2}$ as our unit of length. We then have

$$F=\int d^d x[\tfrac{1}{2}(\nabla\psi)^2-\tfrac{1}{2}\psi^2+\tfrac{1}{4}\psi^4-h\psi] \equiv \int d^d x[\tfrac{1}{2}(\nabla\psi)^2+V(\psi)] . \quad (2.2)$$

The quantity h is a dimensionless measure of the magnetic field or chemical potential. It determines the asymmetry of the potential V. It is sufficient to consider positive values of h. For $0<h<h_0$, where $h_0=2/3\sqrt{3}=0.3849\ldots$ is the classical spinodal value, the potential V (2.2) has, viewed as a function of ψ, an asymmetric double-well structure, with two minima, one at negative $\psi\equiv\psi_-$ and one at positive $\psi\equiv\psi_+$ separated by a maximum at $\psi\equiv\psi_0$. For $h\geq h_0$, only the second minimum survives, while at $h=0$ one recovers the familiar symmetric double-well form. At the classical spinodal $h=h_0$, the values of ψ_- and ψ_0 coincide at $\psi_-=\psi_0=-1/\sqrt{3}$. Clearly the shallow well at $\psi=\psi_-$ is associated with the metastable initial state and the deeper well at $\psi=\psi_+$ with the stable state.

Our objective is to study the time evolution of the system from initial conditions representing the metastable state to the final equilibrium state. The dynamics under which the time evolution takes place is assumed to be given by the Langevin equation

$$\frac{\partial\psi(\mathbf{x},t)}{\partial t}=-\Gamma\frac{\delta F}{\delta\psi(\mathbf{x},t)}+\eta(\mathbf{x},t) , \quad (2.3)$$

where Γ is a dissipative coefficient and $\eta(\mathbf{x},t)$ a Gaussian white-noise field with the strength

$$\langle\eta(\mathbf{x},t)\eta(\mathbf{x}',t')\rangle=2\Gamma\varepsilon\delta(\mathbf{x}-\mathbf{x}')\delta(t-t') . \quad (2.4)$$

Here, the noise strength parameter ε is a dimensionless measure of the temperature. We choose our units of time so that $\Gamma=\frac{1}{2}$. With the units set up in this way, there are two parameters, h and ε, in the problem, and the behavior of the system is to be explored as a function of these two parameters and of the initial conditions which are discussed below.

Our method is to solve (2.3) by numerical integration. The numerical techniques used for the solution and the generation of Gaussian noise are standard and have been thoroughly discussed previously.[9] The system sizes and time ranges required, and other technicalities of this nature, will be given in the next section.

We have focused our study on the time-dependent "magnetization" defined as

$$M(t)=\langle\psi(\mathbf{x},t)\rangle , \quad (2.5)$$

where the brackets denote an average over noise and, where appropriate, also over initial conditions. In practice this average is achieved by solving (2.3) for a sufficient number of "runs" and for each run and time, performing a spatial average and then an average over all runs.

For metastable states which are at least modestly long lived, nucleation phenomena can be studied in terms of the single quantity $M(t)$. This is not the case if we work very close to the classical spinodal.[10] In that case thermal fluctuations of comparatively short duration can attain the size of nucleating droplets, since there is, in this case, a low barrier between the metastable and the stable phases. However, the parameter region explored in our study is sufficiently removed from the spinodal regime so that, as we shall see, the characteristic nucleation time can be unambiguously determined from $M(t)$ alone.

It is worthwhile discussing the expected qualitative behavior of $M(t)$. We treat only sitations where the system is metastable. Thus, we dismiss situations, e.g., $\varepsilon=0$ $\psi(\mathbf{x},t=0)\equiv\psi_-$, where the system does not evolve, and we consider situations in which initially $M(t=0)\approx\psi_-$, and the system then evolves away from the metastable state toward a final equilibrium state near ψ_+. In general, for $\varepsilon>0$, the equilibrium value of M is smaller than ψ_+. We are interested in characterizing the evolution of $M(t)$ from ψ_- to ψ_+ through some characteristic time that can be identified with the time scale for the nucleation of the stable phase. This can be done in several ways. A useful and computationally convenient definition of the characteristic time of this evolution is the time τ when $M(t)$ crosses zero:

$$M(\tau)=0 . \quad (2.6)$$

As our results in the next section show, the region of fastest growth for $M(t)$ is centered in all cases we have studied, around the time region of $t\approx\tau$, with earlier and later time regions showing slower growth. It is therefore sensible to interpret τ as the characteristic time of the nucleation event. Thus, in our data, at times $t=\tau$ the system is irrevocably committed to evolving all the way to the stable state. Note that τ will depend on ε and h, and that the determination of the function $\tau(\varepsilon,h)$ is one of the objectives of this paper.

An alternative definition of the characteristic time, which we will denote here as $\bar{\tau}$ is obtained by determining, at each run, the time at which the site-averaged values of $\psi(\mathbf{x},t)$ equals zero, and then averaging the time values thus obtained over all runs. A moment's thought reveals that one would have $\bar{\tau}=\tau$ if ψ_+ and ψ_- were symmetric with respect to zero. The actual asymmetry

causes $\tilde{\tau}$ to be $\tilde{\tau} \geq \tau$, but the discrepancy is very small. The characteristic time can also be obtained from detailed fits of $M(t)$ to time, as we shall see in the next section.

We must now discuss the initial conditions to be used. Consider first the zero-temperature case ($\varepsilon=0$). If we use the simplest initial condition, $\psi(\mathbf{x},t=0)\equiv\psi_-$, then for $\varepsilon=0$ the system will not change with time and the stable phase will never nucleate. Intuitively speaking one needs, in the absence of noise, to have, in the initial conditions, a sufficiently broad distribution of fields values to ensure that somewhere within the system there will be initial clusters, with field values sufficiently close to those of the stable phase, of sufficiently large size to serve as nucleation centers for the stable phase. In order to achieve this, we work, at $\varepsilon=0$, with random initial conditions for ψ characterized by a Gaussian centered at ψ_- and having a width ε_i which is an additional parameter in the problem. For an infinite system one expects that the stable phase would nucleate somewhere for any finite value of ε_i, no matter how small. In practice, even moderately small values of ε_i require the use of quite large system sizes, as we shall see.

The situation is different when $\varepsilon>0$. In that case the Gaussian noise will eventually cause the stable phase to nucleate since there is always a finite possibility that a nucleating event will eventually occur. It is therefore not necessary to have an initially broadened distribution and, to avoid introducing an additional dimension in our parameter space, we have used the sharp initial distribution $\psi(\mathbf{x},0)\equiv\psi_-$ whenever $\varepsilon>0$. We have also obtained results for an initial distribution $\psi(\mathbf{x},0)\equiv-1$, but these results do not differ in any significant way from those obtained by centering the distribution at the metastable minimum.

Thus, in the next section we will present our results as a function of ε_i and h, at $\varepsilon=0$, and for finite $\varepsilon>0$, as a function of ε and h. We will see that ε and ε_i play, as expected from the above qualitative considerations, a rather similar role.

TABLE I. The parameter values h,ε chosen for study and the resulting values of τ, as defined in (2.6) found in each case.

h	ε	τ
0.15	0.275	246.4
0.15	0.3	137.6
0.15	0.4	37.8
0.2	0.2	209.1
0.2	0.3	35.0
0.2	0.4	19.7
0.25	0.15	103.1
0.25	0.2	37.8
0.25	0.3	18.2
0.25	0.08	168.3
0.3	0.1	60.6
0.3	0.15	24.8
0.3	0.2	17.0
0.35	0.3	194.5
0.35	0.04	61.5
0.35	0.05	39.2
0.35	0.1	17.6
0.35	0.2	10.9

TABLE II. Parameter values h,ε_i studied at $\varepsilon=0$ (see text). The resulting values of τ and the required system sizes are also indicated.

h	ε_i	τ	N
0.25	1.5	136.8	200
0.3	0.7	227.0	400
0.3	0.9	102.7	150
0.3	1.1	59.9	150
0.35	0.3	290.0	600
0.35	0.4	96.4	300
0.35	0.5	88.6	150
0.35	0.7	26.0	150
0.35	0.9	16.3	100

III. RESULTS AND ANALYSIS

The calculations have been performed in a two-dimensional square lattice. In numerical calculations one must necessarily work with a finite system and one must carefully choose the time duration spanned by the calculation. The parameters of the problem must be chosen so that nucleation takes place within this time. The system sizes required in order to have results free of finite-size

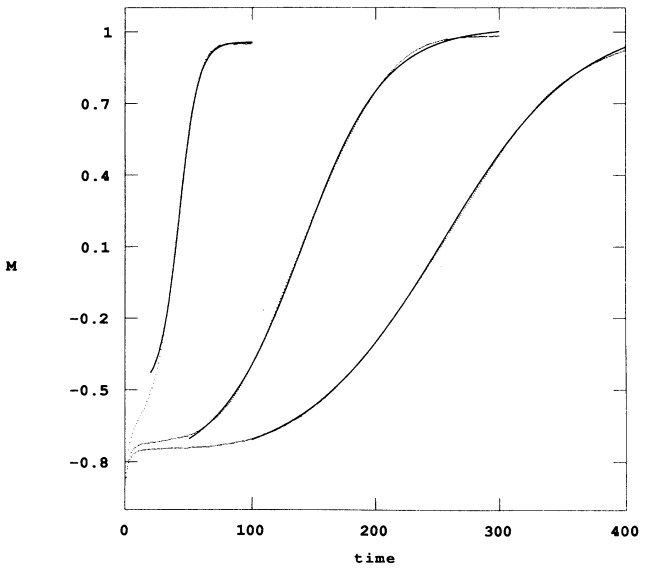

FIG. 1. Results for $M(t)$ vs time for $h=0.15$ and $\varepsilon=0.275$, 0.3, 0.4 (dotted curves from right to left). The solid lines are the fits given by (3.1) with the fitting parameters in Table III. Because of the high quality of the fits, the solid lines partly obscure the dots. $M(t)$ is defined in (2.5).

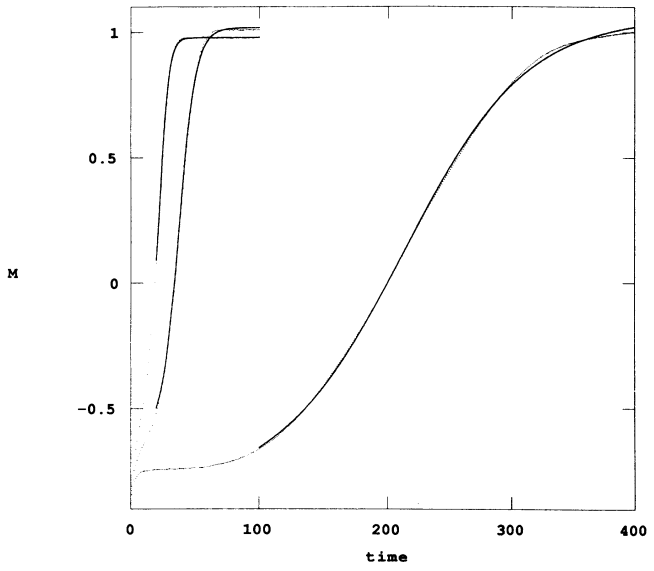

FIG. 2. As in Fig. 1 except for $h=0.2$, $\varepsilon=0.2, 0.3, 0.4$.

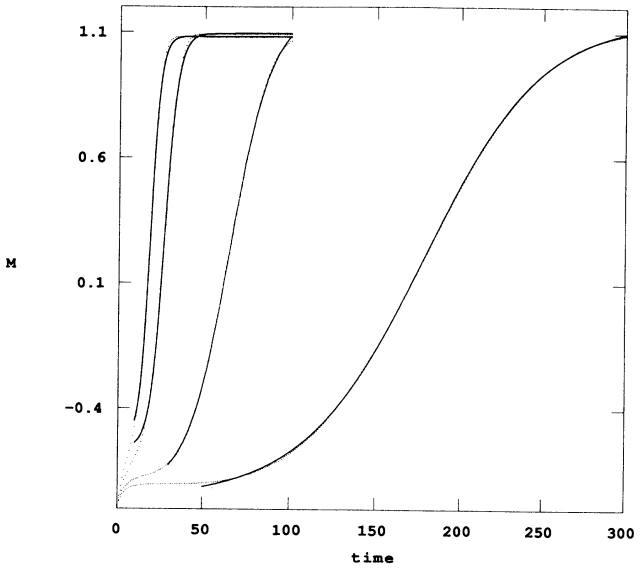

FIG. 4. As in Fig. 1 except for $h=0.3$, $\varepsilon=0.08$ 0.1, 0.15, 0.2.

effects [i.e., to obtain results for $M(t)$ independent of system size] are relatively large which has precluded the use of a three-dimensional lattice. In general, the calculations are carried out to a time sufficiently large that $M(t)$ is at least approaching its equilibrium value. This maximum value of the time is, of course, strongly dependent on the values of h, ε, and, at $\varepsilon=0$, of ε_l. In all cases the results are averaged over a sufficiently large number of runs so that the statistical uncertainty in the values of the characteristic times is smaller than 3%. The number of runs required is usually 20, but 30 are needed for the larger values of the noise parameter. The size N of the $N\times N$ square lattice required for the calculations has been determined by performing trial calculations at progressively larger sizes until the results are clearly size independent. We have found that finite-size effects are not much of a problem for the nonzero values of ε that we have used. A lattice size of $N=150$ is then sufficient in all cases, and the reliable results can be obtained even at $N=100$ whenever the stable phase nucleates relatively quickly. The situation is quite different at $\varepsilon=0$. Then, particularly for smaller values of ε_l, finite-size effects can

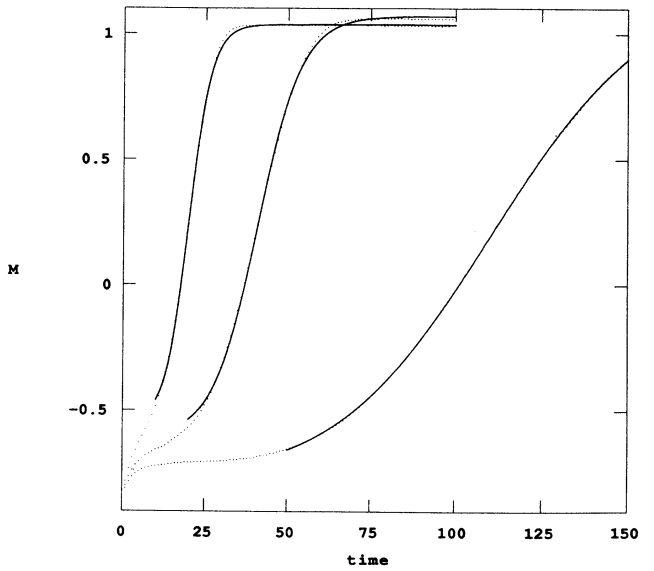

FIG. 3. As in Fig. 1 except for $h=0.25$, $\varepsilon=0.15, 0.2, 0.3$.

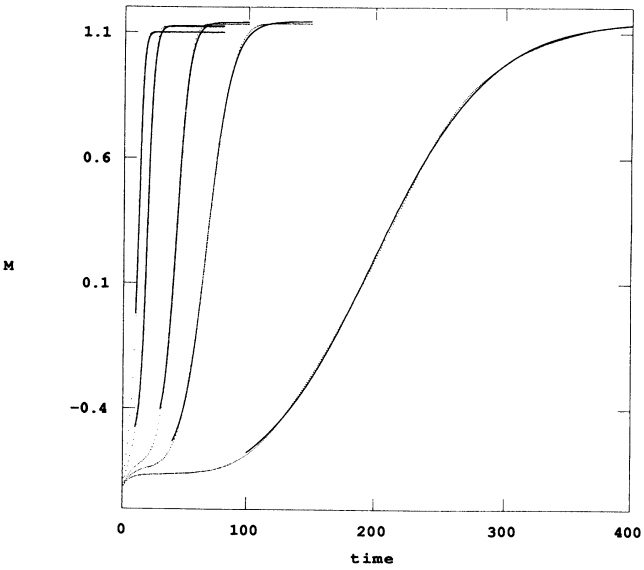

FIG. 5. As in Fig. 1 except for $h=0.35$, $\varepsilon=0.03, 0.04, 0.05, 0.1, 0.2$

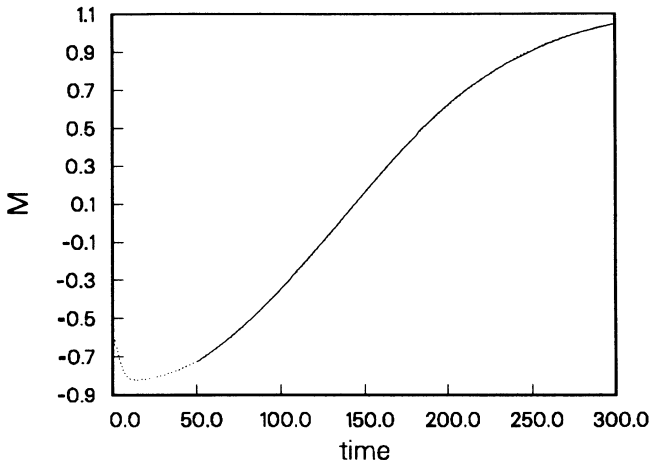

FIG. 6. Results for $\varepsilon=0$. Data for $M(t)$ vs time at $h=0.25$, $\varepsilon_t=1.5$ (dotted line). Again, the solid line that partly obscures the dots is the fit to (3.1), with the parameters given in Table IV.

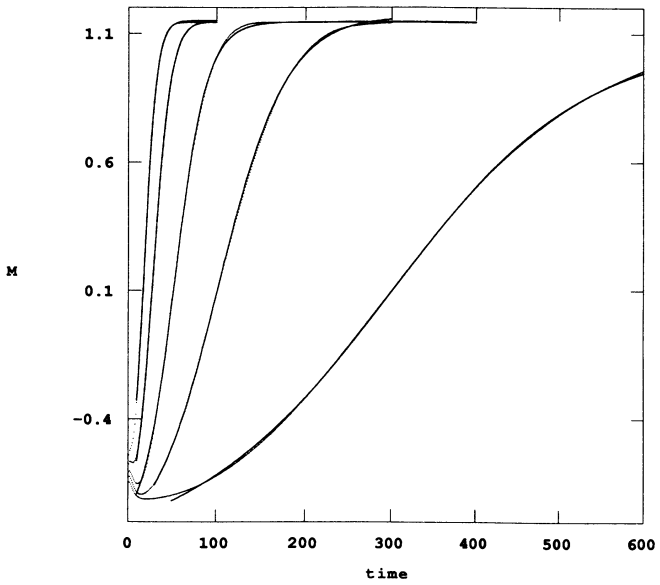

FIG. 8. As in Fig. 6 except for $h=0.35$, $\varepsilon_t=0.3$, 0.4, 0.5, 0.7, 0.9.

be qualitatively quite severe: if N is too small, the system may even simply freeze in the metastable state. Reliable results are not obtained unless N is large enough that the system does not freeze in any of the runs. The sizes required are up to $N=600$.

The values of h, ε, and u employed here are listed in Table I (for $\varepsilon>0$) and Table II ($\varepsilon=0$). In these tables we also indicate the time τ obtained in each case, as determined from (2.8) and, for $\varepsilon=0$, the size N of the system for which they were obtained. For $\varepsilon>0$, satisfactory results could always be obtained for N in the range 100–150. These parameter values span a rather wide region of parameter space. They are clearly away from the spinodal region. Even at $h=0.35$, the largest value of h, one still has well-separated values of ψ_0 and ψ_- (-0.4289 and -0.7140, respectively). We are therefore in the region where a well-defined barrier exists between stable and metastable states. On the other hand, the region explored has been chosen so as to keep the computer times required within the bounds given by available resources. Longer characteristic nucleation times carry with them the need to use considerably larger system sizes. This means leaving the region of very long τ, i.e., lower fields or temperatures, unexplored for the time being.

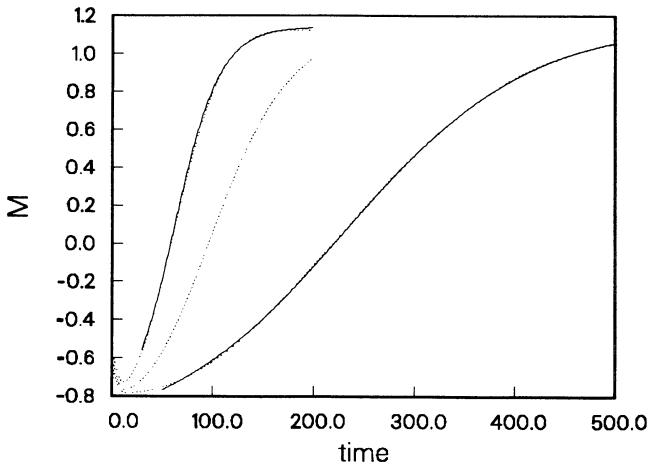

FIG. 7. As in Fig. 6 except for $h=0.3$, $\varepsilon_t=0.7$, 0.9, 1.1 (from right to left). The $\varepsilon_t=0.9$ curve was not fitted, as the data has not saturated for the longest time.

The raw results for $M(t)$ obtained for this choice of parameters are displayed as the dotted lines in Figs. 1–5, which correspond to $\varepsilon>0$, and Figs. 6–8, which are for $\varepsilon=0$. The results for τ in Tables I and II are obtained from precisely the same data (20–30 run averages) as in these figures. The quality of the raw data is evident from the smoothness of the curves. The meaning of the solid lines (which partly obscure the dots) in these figures will be discussed below.

Before proceeding to a quantitative analysis let us comment on the qualitative features of the curves shown in the figures. We see that at early times there is a brief transient. For $\varepsilon>0$, this is characterized by an initial rapid increase, so that $M(t)$ is monotonic throughout the entire time range. For $\varepsilon=0$, $M(t)$ briefly increases (this is barely visible in the figures) and then decreases slightly before beginning to climb again. The exact shape of these transients depends on the details of the initial conditions and we do not think that they are very important. After these transients there is a time region, which depends strongly on ε and h, where $M(t)$ varies quite slowly. Of course, this region is longer at lower temperatures. The values of $M(t)$ in this region are clearly above ψ_-. Subsequently, $M(t)$ increases more rapidly and the nu-

TABLE III. For each pair of values (h,ε), the values of the parameters m_+, a, α, τ [defined in (3.1)] are given. The product $\alpha\tau$ and the fitting range Δt are indicated in the last two columns.

h	ε	m_+	a	α	τ	$\alpha\tau$	Δt
0.15	0.275	1.065	1.30	0.0179	239.4	4.29	100–400
0.15	0.3	1.018	1.24	0.0297	133.0	3.95	50–300
0.15	0.4	0.956	1.90	0.133	37.3	4.96	30–100
0.2	0.2	1.062	1.27	0.0202	199.5	4.03	100–400
0.2	0.3	1.018	1.70	0.152	34.3	5.21	20–100
0.2	0.4	0.979	4.58	0.292	18.5	5.40	20–100
0.25	0.15	1.194	1.53	0.0443	101.2	4.45	50–150
0.25	0.2	1.069	1.77	0.1511	37.1	5.60	20–100
0.25	0.3	1.035	1.89	0.205	17.7	3.62	10–100
0.3	0.08	1.156	1.53	0.0286	163.2	4.67	50–300
0.3	0.1	1.181	1.64	0.0843	59.3	5.00	30–100
0.3	0.15	1.095	1.96	0.257	24.3	6.25	10–100
0.3	0.2	1.083	2.06	0.344	16.6	5.71	10–100
0.35	0.03	1.152	1.53	0.0228	180.9	4.12	100–400
0.35	0.04	1.144	1.82	0.103	61.6	6.34	40–150
0.35	0.05	1.14	2.17	0.199	38.8	7.72	30–100
0.35	0.1	1.125	2.15	0.394	17.0	6.70	10–80
0.35	0.2	1.1	4.06	0.589	10.2	6.01	10–80

cleation of the stable phase begins. The time τ falls, as explained above, in this region of rapid growth. Eventually, $M(t)$ saturates at its final equilibrium value. It is obvious from the figures that, while the qualitative behavior of $M(t)$ is quite general, the values of τ are a very strong function of h, ε, and ε_i. One sees that the characteristic times increase rapidly as ε (or ε_i) decreases and also, at constant ε, when h decreases. This is all as one would expect.

We have fitted the $M(t)$ data curves in Figs. 1–8 to the form

$$M = m_+(1-e^{-\alpha(t-\tau)})/(1+ae^{-\alpha(t-\tau)}) . \tag{3.1}$$

In (3.1) m_+ represents the value of $M(t)$ at long times. The fits are shown as the solid lines in Figs. 1–8. The values of the parameters obtained in the fits are given in Tables III and IV, where we also indicate the time region Δt included in the fit. The initial transient has been excluded. We note that the values at τ obtained from the fits are in very good agreement with the actual values in Tables I and II, and the values of m_+ have the expected temperature dependence. One can see that the fits are extremely good in the intermediate time range and of very good quality at the approach to equilibrium. Thus, (3.1) is a good representation of the overall results.

We now proceed with the analysis of the characteristic time. We will develop this analysis in terms of the values of τ, as given in Tables I and II. The results change very little, and the conclusions not at all, if one uses instead the fitted values of Tables III and IV, or the alternative definition $\tilde{\tau}$, of the characteristic time, as given in the previous section.

In the regime we are considering, where there is a clear separation between the metastable state and the unstable ($\psi \approx \psi_0$) values, it is natural to keep in mind the Becker-Döhring[2] activated form (1.1) for τ. Of course, we expect the activation barrier E to be a function of H, but, at most, a weak analytic[7] function of the reduced temperature ε. The situation for τ_0 is harder to guess. One certainly expects τ_0 to be a function of h. For the temperature dependence, one might expect a temperature independent τ_0 or, possibly, a rate $1/\tau_0$ proportional to $\varepsilon^{1/2}$, reflecting an attempt rate proportional to a thermal ve-

TABLE IV. As in Table III, but at $\varepsilon=0$ with the quantities given as a function of ε_i.

h	ε_i	m_+	a	α	τ	$\alpha\tau$	Δt
0.25	1.5	1.15	1.05	0.0187	134.6	2.52	50–300
0.3	0.7	1.17	1.13	0.0109	220.0	2.40	50–500
0.3	1.1	1.14	1.21	0.0450	58.6	2.64	30–200
0.35	0.3	1.09	1.17	0.0086	277.7	2.39	80–600
0.35	0.4	1.17	1.28	0.0267	94.3	2.52	30–300
0.35	0.5	1.15	1.34	0.0560	47.9	2.68	10–350
0.35	0.7	1.15	1.40	0.1010	25.3	2.56	10–100
0.35	0.9	1.15	1.50	0.1440	15.6	2.25	10–100

TABLE V. For each value of h, the parameters $\tau_0(h)$ and $E(h)$ as defined in (1.1) are given, together with the coefficient of determination of the fit of the data to (1.1). The classical barrier value E_{cl} and its ratio to E are also given. The quantity b is defined in (3.4).

h	τ_0	E	r^2	E_{cl}	E_{cl}/E	b
0.15	0.636	1.63	0.998	9.172	5.63	0.1175
0.2	1.62	0.963	0.990	6.919	7.18	0.0817
0.25	3.07	0.520	0.992	5.325	10.24	0.0507
0.3	3.47	0.30	0.985	4.310	14.32	0.0252
0.35	6.26	0.979	0.984	3.504	35.79	0.006 62

locity. We have performed our fits assuming E to be independent of ε, and for τ_0 both constant or inversely proportional to $\varepsilon^{1/2}$. The latter set of fits turned out in all cases to be of worse quality and will be ignored here. The results are shown in Table V. For the case $\varepsilon=0$, fits of a form similar to (1.1)

$$\tau=\tau_0 e^{E/\varepsilon_t} \tag{3.2}$$

have also been performed. The results are shown in Table VI. We see from this table that the fits are quite good at $\varepsilon=0$, with τ_0 and E both being functions of h and showing the expected trends. On the other hand, it is difficult to reach more general conclusions from the $\varepsilon=0$ results, since we have less data there.

We therefore turn our attention to $\varepsilon>0$ (Table V). We see that there the quality of the fits to the activated form, while improving somewhat at smaller fields, is only adequate at larger fields. The parameters τ_0 and E depend quite strongly on the fields. τ_0 varies by an order of magnitude, and E by a factor of ~ 17 as h varies from 0.15 to 0.35.

For the field values where we have data for a sufficiently large (at least four) number of values of ε, we have found that an excellent fit to the results for τ can be obtained by assuming that E is an analytic function of ε and including in our fitting procedure the coefficients of the first two nonzero powers of ε in the power expansion.

The classical activation energy associated with the creation of a droplet of the stable phase for our problem can be obtained by the two-dimensional analog of the standard calculation described in Ref. 4. One easily obtains, in our units,

$$E_{cl}=\frac{2\pi}{9}\frac{(\psi_+-\psi_-)^2}{|V(\psi_+)-V(\psi_-)|}\ , \tag{3.3}$$

where the potential $V(\psi)$ is defined in (2.2). As $h\to 0$ (3.3) leads to $E_{cl}\sim 1/h$ (in general, $E_{cl}\sim 1/h^{d-1}$ in d dimensions). It should be understood that a constant factor of order unity might exist between the values of the barrier calculated from (3.3) and the measured values due, for example, to differences between the geometrical shape of a droplet on a square lattice and the circular shape assumed in deriving (3.3).

The values of E_{cl} are indicated in Table V. We see that the ratio E_{cl}/E is not a constant, but it increases from 5.63 at $h=0.15$ to 35.79 at $h=0.35$. The change in this ratio does diminish at smaller fields, and one can very tentatively conclude that (3.3) would agree with the computer results in the limit of very small fields.

Monte Carlo simulations for lattice-gas models[10,11] lead, for nucleation near the critical point, to results for the nucleation barrier that are also smaller than the classical values. This seems to be the case for experimental results[12] as well. It has been shown[13] that such a decrease can be explained, for quenches near the critical point, as the result of finite-size effects within the nucleating clusters of the stable phase. These effects lead to a lowering of the bulk part of the free energy for droplets smaller

TABLE VI. As in the first four columns of Table V, for the $\varepsilon=0$ data.

h	τ_0	E	r^2
0.3	5.912	2.557	0.9997
0.35	3.840	1.300	0.9984

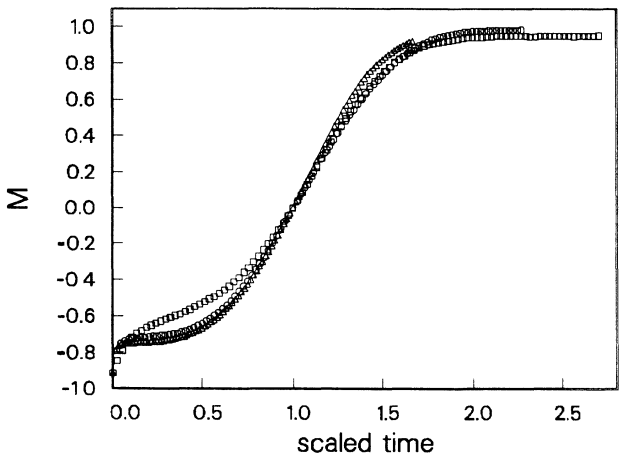

FIG. 9. The data in Fig. 1 replotted in terms of the "scaled time" t/τ. In this and subsequent figures the symbols used (squares, circles, triangles, plus signs, and crosses) denote, in this order, decreasing values of ε or ε_t.

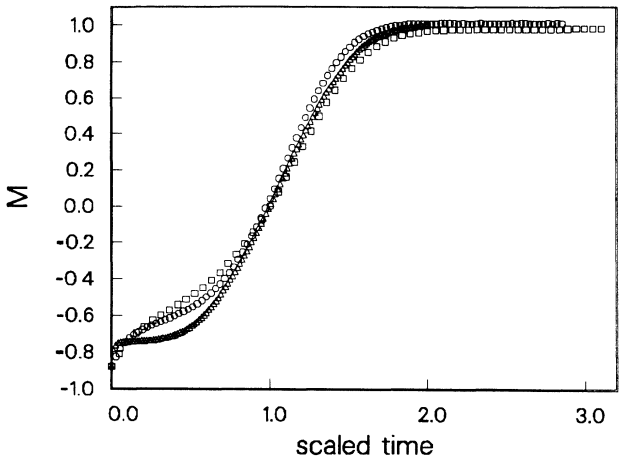

FIG. 10. As in Fig. 9, for the data shown in Fig. 2 ($h=0.2$).

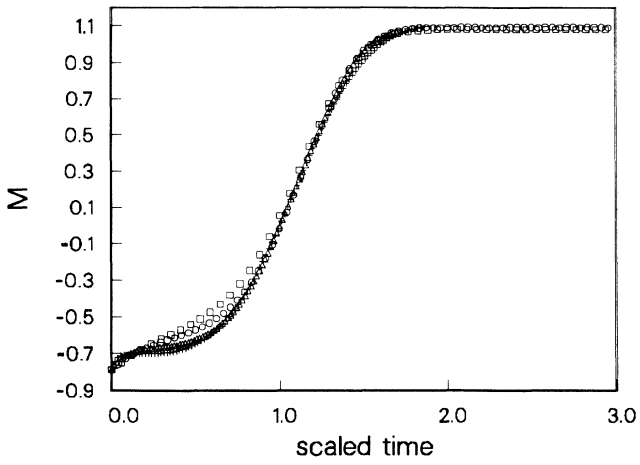

FIG. 12. As in Fig. 9, for the data shown in Fig. 4 ($h=0.3$).

than the correlation length. Our results, however, are obtained well away from the critical region. It appears, therefore, that a more general mechanism must be at work.

Noting from Table V that $E_{\rm cl}$ varies only by a factor of ~ 2.6 over the range of h considered while E, as noted above, varies by a factor of ~ 17 over the same range, one may query whether there is any free-energy barrier in the problem which varies by the required factor over this field range. A rather careful search has unearthed only one candidate, namely,

$$b = |V(\psi_-) - V(\psi_0)| \ . \tag{3.4}$$

This quantity, also listed in Table V, varies by a factor of 17.7 in the range of h considered. The ratio E/b is in the range 10–14 for all fields considered, although it is not precisely a constant. One might, of course, be tempted to interpret this ratio as the "volume" πr^2 of a droplet of the $\psi \equiv \psi_0$ phase of radius $r \sim 2$. Such an argument, although appealing on the grounds that a "droplet" of ψ_0 would evolve towards a value of $\psi = \psi_+$, neglects the surface energy of the boundary separating it from the metastable phase, and one can readily see that such a surface energy term cannot *a priori* be neglected. The formation of a region of $\psi = \psi_0$ with soft walls cannot be ruled out. Overall, we conclude that our nucleation rates are indeed given by an activated form, but that the values of h that we use are beyond the region where the simple formula (3.2) is valid. We note that this intermediate region has been neglected in theoretical work, which has largely concentrated on the classical nucleation region and on the region very near the spinodal.[14]

The results at $\varepsilon = 0$ are consistent with these conclusions with the proviso that the width of the initial conditions, ε_i, plays the role of the temperature. There ap-

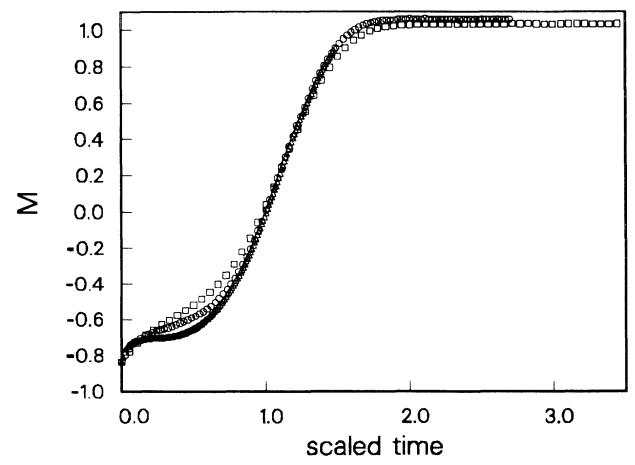

FIG. 11. As in Fig. 9, for the data shown in Fig. 3 ($h=0.25$).

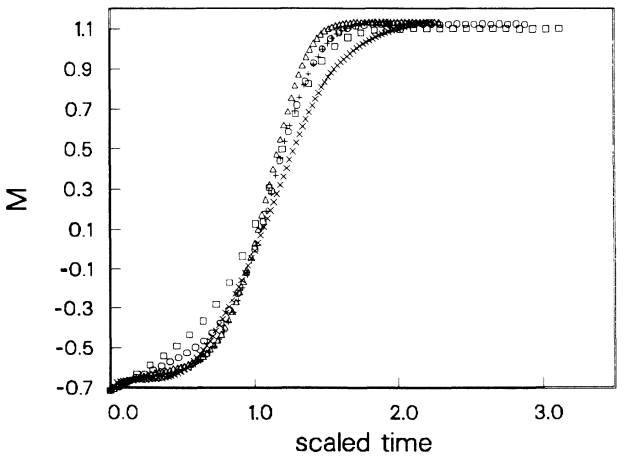

FIG. 13. As in Fig. 9, for $h=0.35$ (data shown in Fig. 5).

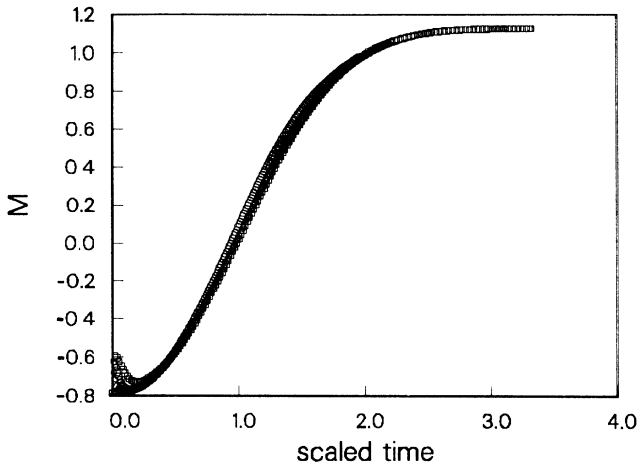

FIG. 14. Similar to Fig. 9, but at $\varepsilon=0$, $h=0.3$ (see Fig. 7).

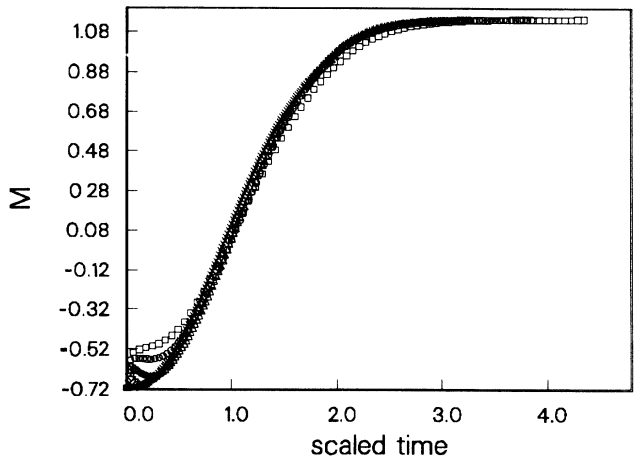

FIG. 15. As in Fig. 14, for $h=0.35$ (data in Fig. 8).

pears to be a large proportionality factor (of order 10) relating an effective temperature ε_{eff} to the parameter ε_i.

We have also plotted our results for $M(t)$ as a function of t/τ. The results are shown in Figs. 9–13 (for $\varepsilon>0$) and Figs. 14–15 ($\varepsilon=0$). We see that, except for the initial transient, the data fall, to reasonable accuracy, on the same curve for a given field regardless of the value of ε (or ε_i). This is rather remarkable, since the data plotted span a rather wide spread set of values of τ. It indicates that ε (or ε_i) controls only the overall time scale and the qualitative behavior of $M(t)$ which is relatively universal.

The behavior shown in these figures can be related to (3.1) which may be written as

$$M=m_+(1-e^{-a\tau(t/\tau-1)})/(1+ae^{-a\tau(t/\tau-1)}) . \quad (3.5)$$

It can be readily seen from Tables III and IV that the parameters a, and $a\tau$ and m_+ are slowly varying functions of ε. Hence, the variable M (or, more accurately M/m_+) is approximately a function of t/τ (the rescaled time) only. This should not be interpreted, of course, as implying that there is a scale-invariant regime, as in symmetric order-growth problems.

In conclusion, we have seen that over the parameter region studied, which is intermediate between the "classical nucleation" and the "classical spinodal" regimes, the nucleation rate is of an activated form. The energy barrier is not given by the result (3.3), but appears to tend towards it in the limit of small fields. The attempt rate is only weakly dependent on the temperature. The region studied is one for which theoretical work is yet to be performed.

ACKNOWLEDGMENTS

This work was supported by the National Science Foundation under Grant No. DMR 87-14707 at the University of Chicago, and by the Cray Research Corporation at the University of Minnesota.

[1]J. Frenkel, *Kinetic Theory of Liquids* (Dover, New York, 1955), Chap. VII.
[2]E. Becker and W. Döring, Ann. Phys. (Leipzig) **24**, 719 (1935).
[3]For a general review see, J. D. Gunton, M. San Miguel, and P. S. Sahni, in *Phase Transitions and Critical Phenomena*, edited by C. Domb and J. L. Lebowitz (Academic, London, 1983), Vol. 8.
[4]J. D. Gunton and M. Droz, in *Introduction to the Dynamics of Metastable and Unstable States*, Vol. 183 of *Lecture Notes in Physics*, edited by J. ZiHartz (Springer-Verlag, Berlin, 1983).
[5]J. W. Cahn and J. E. Hilliard, J. Chem. Phys. **31**, 688 (1959).
[6]J. S. Langer, Ann. Phys. (N.Y.) **41**, 108 (1967).
[7]J. S. Langer and A. J. Schwartz, Phys. Rev. A **21**, 948 (1980).
[8]K. Binder and M. H. Kalos, in *Monte Carlo Methods in Statistical Physics*, edited by K. Binder (Springer-Verlag, Berlin, 1979).
[9]O. T. Valls and G. F. Mazenko, Phys. Rev. B **34**, 7941 (1986).
[10]K. K. Mon and D. Jasnow, Phys. Rev. A **31**, 4008 (1985).
[11]H. Furukawa and K. Binder, Phys. Rev. A **26**, 556 (1982).
[12]E. D. Siebert and C. M. Knobler, Phys. Rev. Lett. **52**, 1133 (1984).
[13]K. K. Mon and D. Jasnow, Phys. Rev. Lett. **59**, 2983 (1987).
[14]L. Monette, W. Klein, M. J. Zuckermann, A. Khadir, and R. Harris, Phys. Rev. B **38**, 11 607 (1988).